Probe Diffusion in Concentrated Polyelectrolyte Solutions: Effect of Background Interactions on Competition between Electrostatic and Viscous Forces

Sidhartha S. Jena*,† and Victor A. Bloomfield

Department of Biochemistry, Molecular Biology and Biophysics, University of Minnesota, 6-155 Jackson Hall, Minneapolis, Minnesota 55455

Received October 1, 2005

ABSTRACT: We have used fluorescence recovery after photobleaching (FRAP) to measure the diffusion coefficient D of a small probe protein, green fluorescent protein (GFP), in solutions of the polyelectrolyte sodium polystyrenesulfonate (NaPSS) over a wide range of conditions. We covered a range of polyelectrolyte concentrations that resulted in solution viscosities η from 1 to 50−100 cP, contrasted the behavior of high molecular weight (1×10^6 Da) and low molecular weight (7×10^4 Da) NaPSS, and explored the effects of low and high salt concentrations. We worked at a solution pH of 5.5, slightly higher than the isoelectric point of the GFP, which therefore had a small net negative charge. We observed positive deviations as large as 10-fold from Stokes−Einstein (S−E) behavior in high molecular weight NaPSS at low ionic strength. However, in low molecular weight NaPSS, approximately the same molecular weight as the DNA from our previous studies, deviations from S−E behavior were more modest, less than 2-fold. For high molecular weight NaPSS at high concentration, D increased with increasing salt concentration while η decreased, indicating a competition between electrostatic force and viscous drag. Fitting of diffusion coefficients to the stretched exponential equation $D/D_0 = \exp(-\alpha c^{\nu})$ yielded values of ν near 1.0 and 0.68 for high and low molecular weight NaPSS solutions, respectively. These observations are consistent with mainly hydrodynamic influences on GFP diffusion in low molecular weight polyelectrolyte, but with increasing importance of electrostatic interactions in high molecular weight NaPSS. Comparisons with previous results show that polyelectrolyte size and flexibility, not just charge and concentration, play major roles in diffusion of probe molecules.

Introduction

The diffusion of macromolecules and proteins in polymer solutions has been studied extensively over the past several years[1−10] because of its importance in a wide variety of applications such as size exclusion chromatography and other separation techniques, biological transport, drug delivery, and flow through gels.

The diffusion coefficient D of a probe particle with hydrodynamic radius R_H is generally analyzed with the Stokes−Einstein (S−E) equation

$$D = \frac{k_B T}{6\pi\eta R_H} \tag{1}$$

where k_B is the Boltzmann constant, T is the temperature, and η is the viscosity of the medium through which the particle is diffusing. A number of experimental studies on probe diffusion in solutions of small molecules with solvent have found that the S−E relation is perfectly obeyed, i.e., $D\eta/(D_0\eta_0) = 1$, where D_0 is the diffusivity of the probe particle in solvent and η_0 is the solvent viscosity.

However, a number of studies on probe diffusion in polymer solutions have found deviations from S−E behavior. A deviation with $D\eta/(D_0\eta_0) > 1$ is usually attributed to the probe experiencing the microviscosity of the solvent rather than the bulk viscosity of the solution, whereas a deviation with $D\eta/(D_0\eta_0) < 1$ is attributed either to particle aggregation or to polymer adsorption on the particles.[11] These deviations signal the breakdown of a basic assumption underlying the S−E equation, that the solvent molecules act as a continuum[12] through which the probe diffuses. This assumption is not valid when the probe size becomes comparable to the correlation length of the polymer solution.[9]

Experimental studies of S−E behavior with charged probes in polyelectrolyte solutions[13−18] are much less common than those with neutral polymers and probes. The dynamical behavior of polyelectrolyte solutions is generally different and more complicated than that of neutral polymer solutions because of long-range interactions and ordering in charged systems.[19] However, most biological polymers are charged, and polyelectrolytes are also used extensively in industry because of their distinctive solution properties, so that such studies are of basic and practical importance.

In biological systems and cells, and also in some nonbiological situations, diffusion takes place in solution environments that are not only highly charged but are also concentrated or crowded. For example, cells generally contain 20−30 wt % of macromolecules and cellular proteins.[20,21] Both charge and concentration will strongly influence diffusion.[22]

In this paper we report studies of the effects of long-range electrostatic interactions on probe diffusion by using charged macromolecules as both background (sodium polystyrenesulfonate, NaPSS) and probe (green fluorescent protein, GFP), controlling the strength of the interaction by varying the salt concentration. We worked at a solution pH of 5.5, slightly higher than the

* To whom correspondence should be addressed. E-mail: sjena@cbs.umn.edu, sid@igcar.ernet.in; Phone: +91-44-27480347; Fax +91-44-27480060; +91-44-27480301.

† Current address: Materials Science Division, Indira Gandhi Center for Atomic Research, Kalpakkam 603 102, India.

10.1021/ma0521304 CCC: $30.25
Published on Web 11/15/2005

isoelectric point of the GFP, which therefore had a small net negative charge. We also studied the effects of crowding by varying the background polyelectrolyte concentration from dilute through semidilute to highly concentrated, from 5 to 100 g/L for high molecular weight NaPSS and from 10 to 500 g/L for low molecular weight NaPSS. We found that the combined effects of charge and crowding cause large positive deviations from S−E behavior, particularly for high molecular weight NaPSS, but the interaction of the two effects was not always predictable.

Materials and Methods

Sample Preparation. The buffer solution with pH 5.5 was made with 10 mM ammonium acetate−HCl in triply distilled deionized water.

Recombinant green fluorescent protein (EGFP, Phe64Leu, Ser65Thr) was purchased from Clon-Tech, Palo Alto, CA, concentrated to 1 mg/mL, stored at −20 °C, and used without any further purification. The GFP probe concentration was kept low enough in all experiments to avoid probe−probe interactions.

Sodium sulfonated polystyrene (NaPSS) of two different molecular weights, 1×10^6 and 7×10^4 Da, was purchased from Aldrich Chemical Co. Inc., Milwaukee, WI (catalog no. 43,457-4 and 24,305-1) and used without further purification.

Polyelectrolyte solutions were prepared by mixing appropriate amounts of the powdered form of NaPSS in triply distilled and deionized water. 2.5 μL of GFP solution at 1 mg/mL was added to 50 μL of polyelectrolyte solution and mixed to uniformity with a vortex mixer.

Fluorescence Recovery after Photobleaching (FRAP). We used FRAP to study the diffusion of probe GFP molecules in strongly interacting NaPSS solutions. A 5 W tunable argon ion laser (model no. 95-3, Lexel Corp., Fremont, CA) operated at 488 nm was used to excite the GFP, which has an excitation maximum around 495 nm and an emission maximum around 520 nm.

A ratio of $10^{-4.4}$ between the probing and bleaching beam intensity in the FRAP experiment was achieved by a combination of an acousto-optic modulator (model no. N35085-3, Neos Technologies, Melbourne, FL) and a set of neutral density filters. The bleaching time for all samples was 350 ms, much less than the characteristic diffusional relaxation time of GFP in the polyelctrolyte solution. A pellicle beam splitter (model no. 37400, Oriel Corp., Stratford, CA) was used to deflect a portion of the laser beam to the photodetector (model no. 822, Newport Instruments) to monitor the stability of the laser power during the time experiments were performed. The rest of the beam was directed to a Nikon Labphot 2 fluorescence microscope by a single beam steering mirror. An iris was attached to the back of the microscope to achieve a well-defined spot size with a sharp contrast between the illuminated and nonilluminated regions. A dichroic mirror (DM 510) was used to direct the laser beam to the sample specimen. The dichroic mirror passes fluorescent light emitted by the sample at wavelengths higher than 510 nm to the photomultiplier tube (PMT) (model no. S982, Hamamatsu, Inc., Bridgewater, NJ) while blocking the incident laser beam.

The sample was injected into a flat capillary microslide of 200 μm inner spacing (catalog no. W-3520-100, Vitrocom, NJ) by capillary action. This produced a uniform thickness of the sample film. Both ends of the flat capillary tube were sealed to avoid flow of the solution during the experiment. In the FRAP experiment the sample microslide was kept on a XYZ movable fluorescence microscope stage. A dichroic mirror was used to direct the fluorescence signal from the sample to the PMT to measure the fluorescent photocurrent. The photocurrent from the PMT was converted to voltage using a 94 K ohm resistive short across the positive and ground terminals of the PMT, and the signal was amplified by a preamplifier (model no. SR560 preamplifier, Stanford Research Systems, Sunnyvale, CA) before being measured and stored to computer disk for later analysis. An A/D converter circuit monitored the voltage (PCI-MIO-16E-4 Multifunction PCI Board, National Instruments, Austin, TX) using Labview (National Instruments) on a personal computer. The laser, optics, and fluorescence microscope were mounted on an optical table for optical stability and vibration isolation.

At high NaPSS concentrations, the FRAP recovery time sometimes exceeded 15−20 min due to high viscosity and slow probe diffusion. To ensure that the probing beam did not bleach the sample over this extended period, we modified the FRAP instrument so that the probe beam could be shuttered to allow an illumination interval as short as 50−60 ms. During longer recovery phases the sample was illuminated for 500 ms at 10 s intervals. For all experiments, the fluorescence signal from the sample was monitored for 60 s with the probing beam before bleaching, to confirm that the probing beam was not bleaching the sample.

The fluorescence recovery curve was fitted to the equation[23]

$$f(t) = \frac{F(t) - F_0}{F^\infty - F_0} = \exp\left(-\frac{2}{1 + 2t/\tau}\right) \tag{2}$$

where $F(t)$ is the fluorescence signal at time t, F_0 is the fluorescence signal just after the bleaching, F^∞ is the fluorescence signal after the recovery is complete, and τ is the diffusional relaxation time of the probe molecule.

The diffusion coefficient D of the probe molecule was determined from τ by the equation

$$D = \frac{r_0^2}{4\tau} \tag{3}$$

where r_0 is the radius of the probing and bleaching spot, found to be 50 μm by optical micrometry.

It was verified experimentally, by placing a thermocouple close to the bleaching and probing spot, that there was no increase in sample temperature during the course of the experiment due to adsorption of energy from high-intensity bleaching beam. All experiments were done at 20 ± 0.2 °C.

The bleaching depth for all the samples was kept between 50 and 60% to get a good signal-to-noise ratio while at the same time achieving a proper recovery curve.[24] For each sample, 10 measurements were done at different XY positions, and an average value of D was obtained. For samples with low viscosity, measurements done at different positions gave highly reproducible results. For high-viscosity preparations, variations up to 15% were observed, probably due to heterogeneity within the sample.

Viscometry. Viscosities of the polyelectrolyte solutions were measured using Cannon-Ubbelohde semi-micro types 50, 75, 100, and 450 viscometers in a water bath kept at 20 ± 0.2 °C. Glycerol and water viscosities were measured using this setup and found to be in excellent agreement with the *CRC Handbook* values.[25] The measurement time for each sample was at least 50 s. The viscosity values were determined by multiple measurements to check the reproducibility of the data. For low NaPSS concentrations the viscosities were highly reproducible, within 1% of each other. For high NaPSS concentrations the viscosities were also high, and multiple measurements typically varied by 5−10%. In those cases, five measurements were made at each concentration, and the mean value was used.

Results

NaPSS Solution Viscosity. The viscosity as a function of polyelectrolyte concentration at three different concentrations of added NaCl, 0, 100, and 200 mM, is shown in Figure 1 for high (1×10^6 Da) and Figure 2 for low (7×10^4 Da) molecular weight NaPSS solutions. Because of its smaller degree of polymerization, we used concentrations of low molecular weight NaPSS as high as 500 g/L, beyond which it was difficult to dissolve the

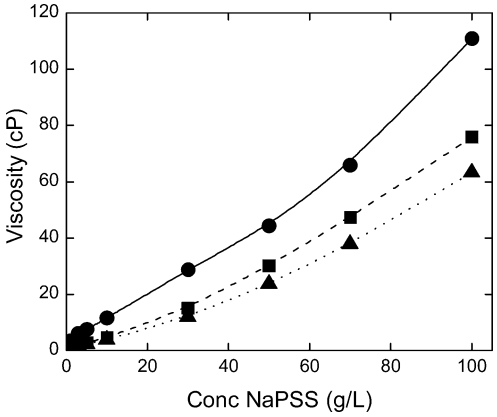

Figure 1. Viscosity of NaPSS ($M_w = 1 \times 10^6$ Da) solutions as a function of concentration at three added NaCl concentrations: (●) 0 mM, (■) 100 mM, and (▲) 200 mM.

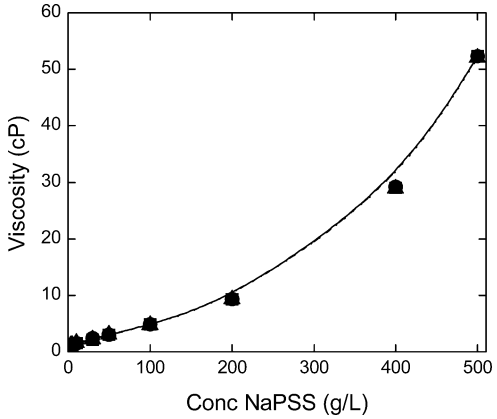

Figure 2. Viscosity of NaPSS ($M_w = 7 \times 10^4$ Da) solutions as a function of concentration at three added NaCl concentrations: (●) 0 mM NaCl, (■) 100 mM NaCl, and (▲) 200 mM NaCl.

polyelectrolyte. Despite this, we could only reach about half the viscosity of high molecular weight NaPSS at its highest concentration, 100 g/L.

The viscosity of the high molecular weight NaPSS solutions decreased upon addition of NaCl due to contraction of the polyelectrolyte chain at high electrolyte concentration.[26] For NaCl concentrations of 500 mM and 1 M (data not shown), the viscosity curves exactly matched, within experimental error, that at 200 mM NaCl. No such variations in viscosity values were observed with addition of NaCl for low molecular weight NaPSS solutions.

Probe Diffusion in High Molecular Weight NaPSS. As NaPSS concentration increases, the solution viscosity increases, so probe GFP diffusion should become slower. At pH 5.5, at which all experiments were performed, NaPSS is fully negatively charged. The probe GFP is also slightly negatively charged, its isoelectric point being 5.1.[27] We therefore expect moderate repulsive electrostatic interactions between background and probe, resulting in effects on diffusion of the probe that will be accentuated at lower screening salt concentration.

Figure 3 shows semilogarithmic plots of the diffusion coefficient D of probe GFP molecules as a function of NaPSS and NaCl concentrations. As expected, D decreases with increasing NaPSS concentration. At higher NaPSS concentrations, D increases with increasing salt, an effect that saturates above 200 mM (data not shown).

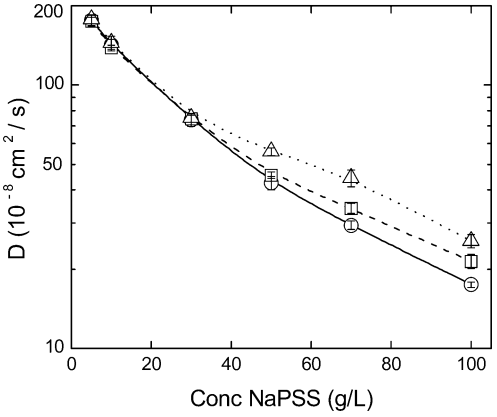

Figure 3. Diffusion coefficient of probe GFP molecules in background NaPSS ($M_w = 1 \times 10^6$ Da) solutions as a function of polyelectrolyte concentrations at three added NaCl concentrations: (○) 0 mM, (□) 100 mM, and (△) 200 mM. D is the same at 500 mM and 1 M NaCl as at 200 mM (data not shown).

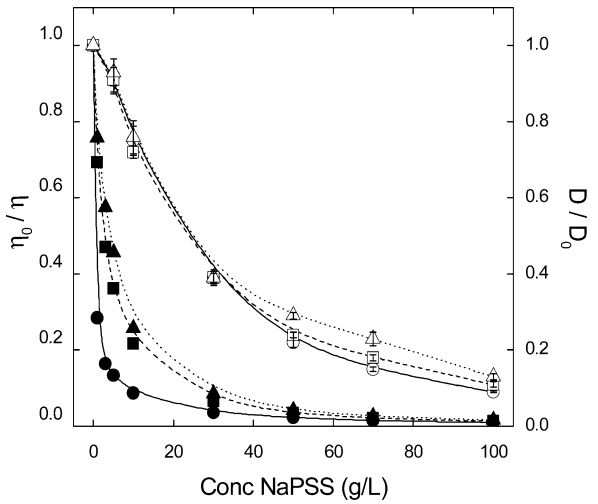

Figure 4. Normalized diffusion coefficient D/D_0 (open symbols, right axis) of GFP in NaPSS ($M_w = 1 \times 10^6$ Da) solutions and inverse normalized viscosity η_0/η (closed symbols, left axis) of NaPSS ($M_w = 1 \times 10^6$ Da) solutions, as a function of polyelectrolyte concentrations at three different NaCl concentrations: (○) 0 mM, (□) 100 mM, and (△) 200 mM.

In Figure 4 we have plotted the normalized GFP diffusion coefficient D/D_0 and inverse normalized solution viscosity η_0/η as functions of NaPSS concentration at three different electrolyte concentrations. The functions do not coincide, indicating that the probe molecules are experiencing a different viscosity than the experimentally measured macroscopic viscosity of the NaPSS solution.

To visualize the deviations from the S−E expectation, we have replotted the data in Figure 4 as $D\eta/D_0\eta_0$ against NaPSS concentration in Figure 5. Deviations from the expected value of 1.0 are greatest at no added salt, but plateau above about 30 g/L NaPSS. For 100 and 200 mM added NaCl, deviations rise steadily until about 70 g/L NaPSS and then level off.

Probe Diffusion in Low Molecular Weight NaPSS. Figure 6 shows D of GFP molecules in low molecular weight ($M_w = 7 \times 10^4$ Da) NaPSS solutions as a function of NaPSS concentration and added salt.

As in high molecular weight NaPSS solutions, D decreased with increase in low molecular weight NaPSS concentration and accompanying solution viscosity. In contrast to the high molecular weight behavior, how-

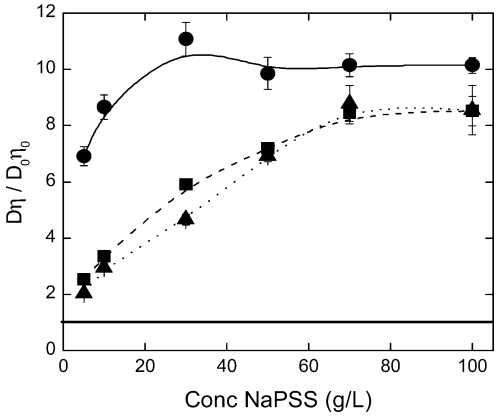

Figure 5. Deviations from Stokes−Einstein relation for GFP diffusion in high molecular weight NaPSS ($M_w = 1 \times 10^6$ Da). The data are plotted as $D\eta/D_0\eta_0$ as a function of NaPSS concentration at three added NaCl concentrations: (●) 0 mM, (■) 100 mM, and (▲) 200 mM. The S−E prediction for the ratio is the horizontal line at 1.0.

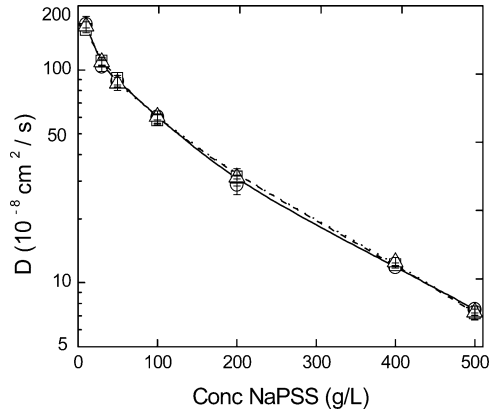

Figure 6. Diffusion coefficient of probe GFP molecules in background NaPSS ($M_w = 7 \times 10^4$ Da) solutions as a function of polyelectrolyte concentrations at three different NaCl concentrations: (○) 0 mM, (□) 100 mM, and (△) 200 mM.

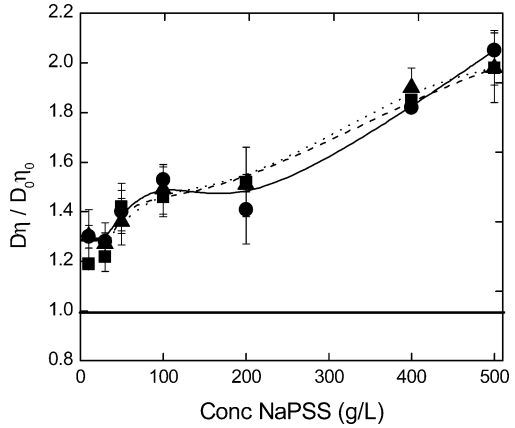

Figure 7. Deviations from Stokes−Einstein relation for GFP diffusion in low molecular weight NaPSS ($M_w = 7 \times 10^4$ Da). The data are plotted as $D\eta/D_0\eta_0$ as a function of NaPSS concentration at three added NaCl concentrations: (●) 0 mM, (■) 100 mM, and (▲) 200 mM. The S−E prediction for the ratio is the horizontal line at 1.0.

ever, D did not change significantly between 0 mM NaCl and 100−200 mM NaCl, echoing the viscosity behavior (Figure 2) in this regard.

Figure 7 shows the Stokes−Einstein plot for diffusion of GFP in low molecular weight NaPSS solutions, combining the data in Figures 2 and 6. Deviations from

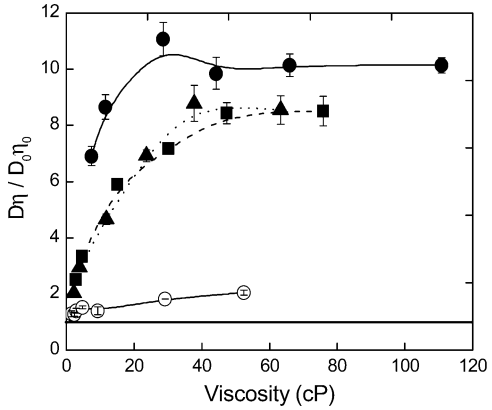

Figure 8. Deviations from Stokes−Einstein relation for GFP diffusion in low (open symbols) and high (closed symbols) molecular weight NaPSS as a function of solution viscosity. The data are plotted as $D\eta/D_0\eta_0$ as a function of NaPSS concentration at three added NaCl concentrations: (●) 0 mM, (■) 100 mM, and (▲) 200 mM. For low molecular weight NaPSS, the three salt concentrations overlap within experimental precision. The S−E prediction for the ratio is the horizontal line at 1.0.

the ideal S−E value of 1 are much smaller than in high molecular weight NaPSS at all concentrations (compare Figure 5, noting different vertical scale), and there is effectively no salt dependence of the deviation.

Viscosity Dependence of Deviations from Stokes−Einstein Behavior. To emphasize the large differences in GFP diffusion between high and low molecular weight NaPSS, in Figure 8 we have plotted $D\eta/D_0\eta_0$ as a function of solution viscosity in both polyelectrolytes. The much greater deviation from S−E expectations in high molecular weight NaPSS at the same viscosity indicates that solution structure, not just bulk viscosity, influences the diffusion of probe molecules in solutions. Figure 8 also emphasizes that electrostatic interactions, as determined by added salt, also play a more significant role with the larger polyelectrolyte.

Stretched Exponential Behavior of Probe Diffusion. Studies of probe diffusion in polymer solutions have frequently observed stretched exponential behavior characterized by eq 4 over a wide range of concentrations.[28]

$$D/D_0 = \exp(-\alpha c^{\nu}) \tag{4}$$

Figures 9 and 10 show our data fit to stretched exponentials for high and low molecular weight NaPSS, respectively.

For high molecular weight polyelectrolyte solution in zero added salt, we found $\nu = 1.02 \pm 0.08$ and $\alpha = 0.027 \pm 0.008$. In 100 and 200 mM NaCl, ν and α were 0.92 ± 0.06 and 0.036 ± 0.01, respectively. In low molecular weight NaPSS solutions at all salt concentrations, ν and α were 0.68 ± 0.03 and 0.05 ± 0.007, respectively.

Discussion

This study is a continuation of work in our laboratory[29,30] in which we have used the fluorescence recovery after photobleaching technique (FRAP) to investigate the dynamics of a protein diffusing in a crowded, strongly interacting macromolecular environment. In the earlier work our focus was on relatively short, persistence length DNA (ca. 10^5 Da) as the background polyelectrolyte. Perhaps the most striking finding was

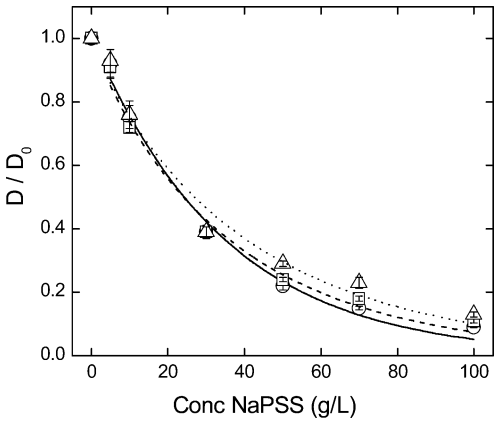

Figure 9. Ratio of D for GFP at finite NaPSS ($M_w = 1 \times 10^6$ Da) concentrations to D_0 at zero NaPSS as a function of polyelectrolyte concentration at three added NaCl concentrations: (○) 0 mM, (□) 100 mM, and (△) 200 mM. The lines are fits to the stretched exponential equation (4). See text for fitting coefficients.

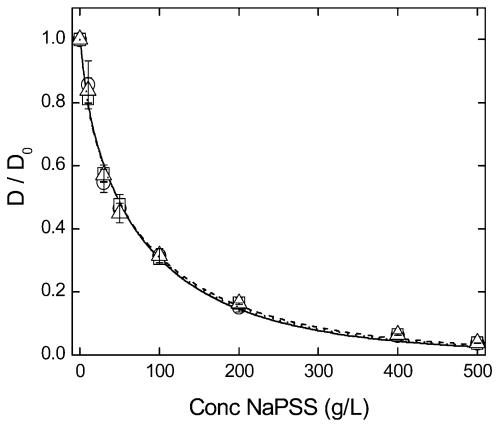

Figure 10. Ratio of D for GFP at finite NaPSS ($M_w = 7 \times 10^4$ Da) concentrations to D_0 at zero NaPSS as a function of polyelectrolyte concentration at three added NaCl concentrations: (○) 0 mM, (□) 100 mM, and (△) 200 mM. The lines are fits to the stretched exponential equation (4). See text for fitting coefficients.

the observation of strong positive deviations (as much as 5-fold) from the Stokes−Einstein (S−E) equation in DNA solutions at low ionic strength.[30] We wished to determine whether this behavior would also be observed in other polyelectrolyte solutions.

In the present work we have measured diffusion of a small probe protein, green fluorescent protein (GFP), in solutions of the polyelectrolyte sodium polystyrenesulfonate (NaPSS) over a wide range of conditions. We covered a range of polyelectrolyte concentrations that resulted in solution viscosities from 1 to 50−100 cP, contrasted the behavior of high molecular weight (1×10^6 Da) and low molecular weight (7×10^4 Da) NaPSS, and explored the effects of low and high salt concentrations. Again, perhaps the most striking finding was even larger (as much as 10-fold) positive deviations from S−E behavior in high molecular weight NaPSS at low ionic strength. However, we found that in low molecular weight NaPSS, approximately the same molecular weight as the DNA from our previous studies, deviations from S−E behavior were more modest, less than 2-fold. Evidently, polyelectrolyte size and flexibility, not just charge and concentration, play major roles in diffusion of probe molecules.

Deviations from S−E behavior have been observed in many polymer solutions and are usually explained by the concept of microviscosity, in which the probe particle samples a volume where the viscosity is different from the experimentally measured bulk or macroscopic viscosity. Typically, such a region will have a low polymer concentration and therefore a viscosity close to that of the solvent. The effect would therefore be expected to depend on polymer size (the domain occupied by an individual polymer coil) and concentration. If the background polymer is a polyelectrolyte, then its domain will be expanded at low screening electrolyte concentration, potentially amplifying the positive deviations from S−E behavior.

These expectations are generally borne out in our experiments. At the same viscosity, the S−E parameter is much greater for high molecular weight than for low molecular weight NaPSS (Figure 8). For example, in low salt at a solution viscosity of 50 cP, D(high) ≈ 35 while D(low) ≈ 7. This means that D is higher in high molecular weight NaPSS, consistent with the idea that there are greater voids in the high molecular weight solution, so the GFP is sampling more free solvent space (microviscosity). For high molecular weight NaPSS, low NaCl leads to increasing viscosity (Figure 1) and decreasing diffusion (Figure 3), but an increasing S−E parameter (Figure 5); D does not decrease as much as would be predicted from η. If one assumes that decreasing NaCl swells the NaPSS, thereby increasing η, it may be thought to both distribute obstacles to GFP diffusion more broadly (less opportunity to squeeze between NaPSS molecules or blobs), but also to allow GFP to diffuse within molecular domains of NaPSS. The S−E parameter levels off at about 50 g/L, suggesting that the two effects compensate or saturate above that concentration.

In low molecular weight NaPSS solutions, D decreases with increasing polyelectrolyte concentration (Figure 6) as viscosity increases (Figure 2), but the deviation from S−E expectation is much less than in high molecular weight solutions (Figure 8) although the deviation increases with increasing NaPSS concentration (Figure 7). Furthermore, D, η, and the S−E ratio do not change significantly with added salt in low molecular weight NaPSS, in contrast to the behavior in high molecular weight polyelectrolyte.

In fact, diffusional behavior of GFP in low molecular weight NaPSS is similar to that in the neutral polymer Ficoll 70, which is of similar size.[30] It appears that the chain expansion of the low molecular weight NaPSS is not much affected by ionic strength, and the average distance between chains is the main factor affecting probe diffusion. This behavior is notably different from GFP diffusion at low salt in persistence length DNA, also of similar size to low molecular weight NaPSS, where the ordinary−extraordinary transition of the DNA couples to the probe dynamics to give larger S−E deviations.[30] The electrostatic coupling was undoubtedly stronger in our DNA experiments, conducted at pH 7, than in the NaPSS experiments at pH 5.5 because the GFP, with isoelectric pH 5.1, would have been more strongly negatively charged at the higher pH. We see further examples of this in the accompanying paper.[32]

The stretched exponential parameters (eq 4) were also noticeably different in high and low molecular weight NaPSS solutions. The high molecular weight values, with ν near 1.0 and α near 0.03, are similar to those

obtained in this laboratory for the diffusion of GFP and BSA-FITC in persistence length DNA solutions at zero salt.[29,30] In low molecular weight NaPSS, we observed lower values of ν and higher values of α. A survey[31] of a wide range of experiments on biological, natural, and synthetic polymer solutions found values of ν ranging from 0.5 to 1, with lower values interpreted as arising primarily from hydrodynamic interactions and higher values from electrostatic interactions. Our results seem consistent with these interpretations.

Acknowledgment. This research was supported in part by grants from NIH (GM28093) and NSF.

References and Notes

(1) Furukawa, R.; Arauz-Lara, J. L.; Ware, B. R. *Macromolecules* **1991**, *24*, 599−605.
(2) Bu, Z.; Russo, P. S.; Tipton, D. L.; Negulescu, I. I. *Macromolecules* **1994**, *27*, 6871−6882.
(3) Nemoto, N.; Kojima, T.; Inoue, T.; Kishine, M.; Hirayama, T.; Kurata, M. *Macromolecules* **1989**, *22*, 3793−3798.
(4) Brown, W.; Pu, Z. *Polym. Rev.* **1990**, *31*, 772−777.
(5) Phillies, G. D. J. *J. Phys. Chem.* **1989**, *93*, 5029−5039.
(6) Cao, X.; Bansil, R.; Gantz, D.; Moore, E. W.; Niu, N.; Afdha, N. H. *Biophys. J.* **1997**, *73*, 1932−1939.
(7) Bu, Z.; Russo, P. S. *Macromolecules* **1994**, *27*, 1187−1194.
(8) Wheeler, L. M.; Lodge, T. P. *Macromolecules* **1989**, *22*, 3399−3408.
(9) Ye, X.; Tong, P.; Fetters, L. J. *Macromolecules* **1998**, *31*, 5785−5793.
(10) Feder, T. J.; Brust-Mascher, I.; Slattery, J. P.; Baird, B.; Webb, W. W. *Macromolecules* **1996**, *29*, 2767−2773.
(11) Won, J.; Onyenemezu, C.; Miller, W. G.; Lodge, T. P. *Macromolecules* **1994**, *27*, 7389−7396.
(12) Einstein, A. In *Investigations on the Theory of Brownian Movement*; Dover Publications: New York, 1956; p 122.
(13) Gorti, S.; Ware, B. R. *J. Chem. Phys.* **1985**, *83*, 6449−6456.
(14) Phillies, G. D.; Malone, C.; Ullmann, K.; Ullmann, G. S.; Rollings, J.; Yu, L. *Macromolecules* **1987**, *20*, 2280−2289.
(15) Dunstan, D. E.; Stokes, J. *Macromolecules* **2000**, *33*, 193−198.
(16) Tanahatoe, J. J.; Kuil, M. E. *J. Phys. Chem. B* **1997**, *101*, 10839−10844.
(17) Bremmell, K. E.; Dunstan, D. E. *Macromolecules* **2002**, *35*, 1994−1999.
(18) Sehgal, A.; Serry, T. A. P. *Macromolecules* **2003**, *36*, 10056−10062.
(19) Krause, W. E.; Tan, J. S.; Colby, R. *J. Polym. Sci., Part B: Polym. Phys.* **1999**, *37*, 3429−3437.
(20) Fulton, A. B. *Cell* **1982**, *30*, 345−347.
(21) Han, J.; Herzfeld, J. *Biophys. J.* **1993**, *65*, 1155−1161.
(22) Kozer, N.; Schreiber, G. *J. Mol. Biol.* **2004**, *336*, 763−774.
(23) Jacobson, K.; Wu, E.; Poste, G. *Biochim. Biophys. Acta* **1976**, *433*, 215−222.
(24) Meyvis, T. K. L.; De Smedt, S. C.; Van Oostveldt, P.; Demeester, J. *Pharm. Res.* **1999**, *16*, 1153−1162.
(25) Weast, R. C.; Astle, M. J. *CRC Handbook of Chemistry and Physics*; CRC Press: Boca Raton, FL, 1985.
(26) In *Polyelectrolytes*, Hara, M., Ed.; Marcel Dekker: New York, 1993.
(27) In *Green Fluorescent Protein: Properties, Applications and Protocols;* Chalfie, M., Kain, S., Eds.; Wiley: New York, 1998.
(28) Phillies, G. D. J. *Macromolecules* **1986**, *19*, 2367.
(29) Wattenbarger, M. R.; Bloomfield, V. A.; Bu, Z.; Russo, P. S. *Macromolecules* **1992**, *25*, 5263−5265.
(30) Busch, N. A.; Kim, T.; Bloomfield, V. A. *Macromolecules* **2000**, *33*, 5932−5937.
(31) Dwyer, J. D.; Bloomfield, V. A. *Biophys. Chem.* **1995**, *57*, 55−64.
(32) Jena, S. S.; Bloomfield, V. A. *Macromolecules* **2005**, *38*, 10557−10560.MA0521304

MA0521304